Gas content effect on bubble motion

Bo Yang (杨 波)[1], **Xiao Chen (陈 笑)**[2], **Rongqing Xu (徐荣青)**[3], **Jian Lu (陆 建)**[1], **and Xiaowu Ni (倪晓武)**[1]

[1] *Department of Applied Physics, Nanjing University of Science and Technology, Nanjing 210094*

[2] *School of Physics, Peking University, Beijing 100871*

[3] *School of Electronics and Information Engineering, Jiangsu University of Science and Technology, Zhenjiang 212003*

The gas content is one of the important bubble parameters. In this article, the gas content effect on the bubble motion is investigated by numerical simulation based on the spherical bubble model. The dependence of the bubble radius, oscillation velocity and the corresponding bubble energy on the gas content during the bubble pulsation is analyzed in detail according to differential equations of the bubble dynamics. The numerical calculations are shown that with the gas content remained in a cavity increasing, the corresponding bubble radii become larger. Further, both the maximum bubble radius and bubble energy show approximately linear-relation with the gas content during the first oscillation cycle, while in the second pulsation period they are observed non-linear with the gas content. In addition, with the gas content increasing, the bubble expanding and contracting velocities are both decreased, whereas the corresponding oscillation periods at the first two oscillations are obviously prolonged.

OCIS codes: 000.4430, 140.3390.

Pulsed laser processing of materials, as an important laser application, has attracted much interest since 1960. The fundamental research on laser processing of air, including its theory and processing technologies, has continued to develop. Lately in laser medicine, laser–matter interaction underwater needs to be studied because most biological tissues and fluids contain more than 85% water[1−5]. When a laser pulse is focused into a liquid, it induces optical breakdown through nonlinear absorption, which leads to plasma formation at the laser's focus. Plasma expansion is always accompanied by the emission of shock waves and the generation of cavitation bubbles[6,7]. Herring[8] analyzed the pressure variation in bubble and introduced first-order correction for liquid compressibility when researching on the explosion under water in 1941. Trilling[9] generalized Herring's research for velocity and pressure in the flow field and calculated the qualification of bubble collapse. Their research method is the quasi-acoustic approximation. Since the first measurement by Bell and Landt[10], various measurement techniques, including highspeed photography[7,11], interferometry[12], optoacoustic detection[13] and mechanical methods[14], have been developed. In this article, the analysis model of bubble including the gas content based on the approximation. Then experimental principle and result are given and then compare with numerical simulation.

We used the quasi-acoustics approximate expression and the expression of pressure at the bubble wall to calculate the relation between gas content and the bubble radius. The model considers the compressibility of the liquid surrounding the bubble and the gas content effect on bubble motion. Otherwise, it is considered that the surface tension and the viscosity of liquid cause to the energy dissipation. The bubble dynamics is described by the quasi-acoustic equation

$$R \cdot \ddot{R} \cdot (1 - \frac{2\dot{R}}{C}) + \frac{3}{2}\dot{R}^2(1 - \frac{4}{3} \cdot \frac{\dot{R}}{C}) = \frac{1}{\rho_0}\left[\frac{R}{C} \cdot \frac{\mathrm{d}P(R,t)}{\mathrm{d}t} + P(R,t) - P_0\right], \quad (1)$$

where, R is the radius of the bubble, $\dot{R} = \frac{\mathrm{d}R}{\mathrm{d}t}$ is the bubble wall velocity. The term $\ddot{R} = \frac{\mathrm{d}^2R}{\mathrm{d}t^2}$ is the acceleration of bubble wall. C is the speed of sound in the liquid. The symbol P_0 is the standard pressure of infinite distance to the bubble.

Assuming ideal gas inside the bubble, the pressure $P(R,t)$ at the bubble wall is given by

$$P(R,t) + \frac{4\eta\dot{R}}{R} + \frac{2\sigma}{R} = kP_0\left(\frac{R_0}{R}\right)^{3\gamma}, \quad (2)$$

where k is the gas content in bubble, η is the coefficient of viscosity, σ is the surface tension. γ is the ratio of specific heat. The pressure $P(R,t)$ is assumed to be uniform throughout the volume of the bubble, where the pressure inside the bubble equals the hydrostatic pressure. By the onward and backward finite difference expression which can be deduced from Eqs. (1) and (2), bubble radius in optional hour can be calculated if the maximum bubble radius in the first oscillation cycle and the corresponding hour are measured from experiment. Based on Rayleigh[15] equation,

$$R\ddot{R} + \frac{3}{2}\dot{R}^2 = -\frac{P_\infty}{\rho}. \quad (3)$$

The bubble energy with the maximum bubble radius

$$E_\mathrm{b} = \frac{4}{3}\pi P_0 R_{\max}^3, \quad (4)$$

where, $R_{\max}$ is the maximum bubble radius.

In Fig. 1 we present a schematic representation of the experiment equipment used to measure shock wave and bubble motion based on light deflection.

With the variation of detection range, sequence waveform of laser plasma bubble, bubble expanding period and contracting period can be obtained in the experiment. From these, the bubble radius alteration with time can be deduced. In Fig. 2, it shows three complete oscillation periods which circles are the average value of data in five experiments and curve is the result of numerical

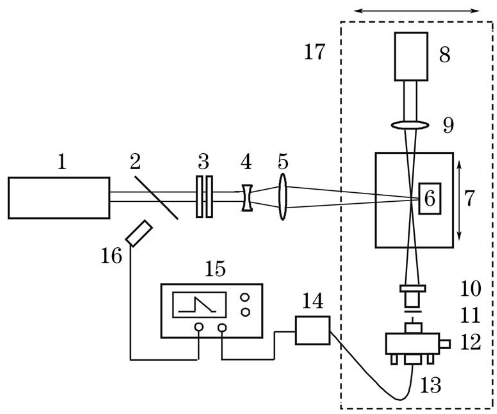

Fig. 1. Experimental equipment abridged general view. 1, Q-switched Nd:YAG laser (wavelength, 1.06 μm; pulse duration, 10 ns); 2, beam splitter; 3, attenuator group; 4, concave lens (f=50 mm); 5, convex lens (f=150 mm); 6, aluminum target; 7, glass cuvette; 8, He-Ne laser (power, 5 mW; wavelength, 0.63 μm); 9, convex lens (f=50 mm); 10, microscope objective (20×, f= 4 mm); 11, interference filter (central wavelength, 0.63 μm); 12, five-axis fiber chuck positioner (0.1-μm spatial resolution); 13, single-mode optical fiber; 14, photomutiplier (Hamamatsu 5773 with 2-ns rise time); 15, digital oscilloscope (Tektronix TDS340); 16, PIN photodiode (0.1-ns rising edge); 17, two-dimensional platform (10-μm spatial resolution).

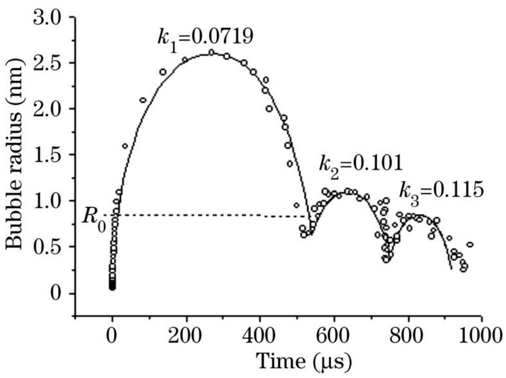

Fig. 2. The variation of bubble radius with time.

simulation based on the onward and backward finite difference equation.

In the last two oscillation periods, the randomness of experiment data is greater than the first oscillation periods. From this figure, the maximum and minimum bubble radius even oscillation periodic time can be determined in every oscillation periods. Based on Eq. (4), the bubble energy in every oscillation periods is also calculated. The bubble characteristic parameters are listed in Table 1.

In this Table, we can conclude that the maximum bubble radius, the minimum bubble radius, minimum bubble radius and periodic time in every oscillation decrease with increasing of the number of oscillation. In the first two oscillation, the attenuation amplitude of characteristic parameter exceeds 50%. In the same oscillation periods, the bubble contracting velocity is much quicker than the bubble expanding velocity especially for collapsing anaphase. Considering that there exist viscosity of fluid and shockwave because of bubble collapse and jet current, the bubble energy dissipates in vast scale. In the whole bubble motion, the bubble energy centralizes in the first oscillation, therefore bubble motion affecting surrounding flow field such as cavitation erosion centralizes in the first oscillation. The gas content is the important characteristic parameter effecting on the bubble motion. It influences the bubble radius, periodic time, expanding and contracting velocity. In this article, we calculate the variation of gas content in the first three oscillations. The gas content k_1 is equal to 0.0719 in the first oscillation. In the second and the third oscillation, gas contents are equal to 0.101 and 0.115 respectively.

From these results, the gas content in every oscillation presents the increasing tendency; on the contrary, the amplitude presents the decreasing tendency. In the first two oscillations, the average amplitude of gas content is about 140%, while 114% in the last two oscillations. In the process of bubble motion, the variation of gas content is determined by the inward-outward pressure difference. Because of the inward pressure is higher than outward pressure in the first stage of expanding, the bubble expands in the pressure difference. With expanding of bubble, the inward pressure decreases continuously. When the inward pressure is equal to outward pressure, the bubble radius is the equilibrium radius and then the expanding velocity reaches the maximum value. Because of the inertia of bubble motion, bubble continues expanding process until reaching the maximum bubble radius. Then the outward pressure is higher than the inward pressure, so the contracting period begins. With the inward pressure increasing continuously, bubble continues to extract and the inward pressure is equal to the outward pressure, that is, the equilibrium radius. Because of the inertia of liquid motion, the bubble motion extracts exceedingly until reaching the minimum bubble radius. This is the first bubble motion cycle. Considering the variation of gas content is depended upon the inward-outward pressure difference, the equilibrium radius is characteristic identification of gas content increase and decrease. When bubble radius is less than the equilibrium radius, the gas content decreases because the inward pressure is higher than outward pressure and gas leak through the bubble wall. On the contrary, the gas content increases. The equilibrium radius is an important characteristic parameter describing the bubble motion.

Table 1. The Bubble Characteristic Parameters

	The First Oscillation	The Second Oscillation	The Third Oscillation
Maximum Bubble Radius $R_{\max}$ (mm)	2.60	1.10	0.85
Minimum Bubble Radius $R_{\min}$ (mm)	0.63	0.36	0.25
Oscillation Periodic Time T (μs)	540	208	170
Bubble Energy E (mJ)	7.34	0.56	0.26

According to the equilibrium radius corresponding to the maximum velocity of bubble motion, the equilibrium radius can be deduced by the onward and backward difference equation. In the first oscillation, the corresponding equilibrium radius is 0.84 mm. Corresponding to time in Fig. 2, the state which the inward pressure is less than the outward pressure, that means negative pressure in a bubble, spends on the majority of the first oscillation periodic time (95%). In the real process, the gas infiltration capacity is higher than the gas seepage. Therefore, the gas content increases gradually with increasing the oscillation number. Because the periodic time decreases, the oscillation amplitude decreases.

In conclusion the numerical simulation disclosures gas content increases the elastic behavior of bubble at the same bubble energy. The gas content is higher, the extracting process prolongs. Bubble energy and the gas content are the competitive relation in bubble motion.

X. Ni is the author to whom the correspondence should be addressed, his e-mail address is nxw@mail.njust.edu.cn.

References

1. J. C. Miller and D. B. Geohegan, *Laser ablation: Mechanisms and Application* (American Institute of Physics, New York, 1994).
2. K. Obata, K. Sugioka, T. Akane, N. Aoki, K. Toyoda, and K. Midorikawa, Appl. Phys. A **73,** 755 (2001).
3. B. N. Chichkov, C. Momma, S. Nolte, F. von Alvensleben, and A. Tünnermann, Appl. Phys. **63,** 109 (1996).
4. R. C. Issac, P. Gopinath, G. K. Varier, V. P. N. Nampoori, and C. P. G. Vallabhan, Appl. Phys. Lett. **73,** 163 (1998).
5. M. H. Niemz, *Laser-Tissue Interactions: Fundamentals and Application* (Springer-Verlag, Berlin, 1996) P156.
6. A. Vogel, S. Busch, and U. Parlitz, J. Acoust. Soc. Am. **100,** 148 (1996).
7. C. D. Ohl, T. Kurz R. Geislier, O. Lindau, and W. Lauterborn, Phil. Trans. R. Soc. London Ser. A **357,** 269 (1999).
8. C. Herring, *Theory of the Pulsation of the Gas Bubble Produced by an Underwater Explosion.* (Columbia University. Press, New York, 1941)
9. L. Trilling. J.Appl.Phys. **23,** 14(1952).
10. C. E. Bell and S. A. Landt, Appl. Phys. Lett. **10,** 46 (1967).
11. A. Vogel, W. Lauterborn, and R. Timm, J. Fluid Mech. **206,** 299 (1989).
12. B. Ward and D. C. Emmony, Appl. Phys. Lett. **59,** 2228 (1991).
13. A. G. Doukas, A. D. Zweig, J. K. Frisoli, R. Birngruber, and T. F. Deutsch, Appl. Phys. B **53,** 237 (1991).
14. H. Schoeffmann, H. Schmidt-Kloiber, and E. Reichel, J. Appl. Phys. **63,** 46 (1988).
15. R. Lord, Philos. Mag. **34,** 94 (1917).